Electrodeposition, structural, and corrosion properties of Cu films from a stable deep eutectics system with additive of ethylene diamine

Gu Changdong, You Yihui, Wang Xiuli, Tu Jiangping
(Department of Materials Science and Engineering, Zhejiang University, HangZhou 310025)

Abstract: A comparative study was carried out on the deposition mechanism, microstructure, and corrosion resistance of Cu films electrodeposited from the base electrolyte of CuCl2·2H2O in a choline chloride ─ethylene glycol eutectic solvent with absence and presence of the additive of ethylene diamine (EDA). The base electrolyte is unstable and produces rough Cu films with columnar grains. Upon the introduction of EDA, the modified electrolyte becomes stable and the nucleation of Cu deposits is strongly inhibited, thus producing a smooth and compact surface with finer grains. Uniform corrosion and decreased corrosion current density are recognized in the fine grained Cu films.

Keywords: Electrodeposition; Ionic liquids; Copper; Additive; Corrosion resistance

0 Introduction

Electrodeposition of copper is widely adopted in the electronics industry for production of printed circuit boards, selective case hardening of steel for engineering components, and production of electrotypes in the printing industry due to its lower electrical resistivity compared to aluminum and decorative appearance [1-4]. Particularly, copper can act as a protective layer to magnesium alloys and zinc alloy die-castings to allow further coatings to be applied [1, 5]. Moreover, as the grain size reduces into the nanometer range, metals usually exhibit peculiar and interesting mechanical and physical properties, e.g. increased mechanical strength, enhanced diffusivity, and higher specific heat compared to conventional coarse grained counterparts [6, 7]. Interestingly, when the grain size is characterized by a bimodal grain size distribution, i. e. with micrometre-sized grains embedded inside a matrix of nanocrystalline and ultrafine grains, Cu samples would exhibit an optimized mechanical property with a high tensile ductility and high strength [8]. High corrosion resistance is also found for the nanocrystalline metals [9-12]. The commercial copper electroplating is largely based on the toxic cyanic or phosphate electrolytes. Complexing agents such as citrate, thiocyanate, and pyrophosphate have been sought as both environment and hazards safe alternatives [13, 14]. Obviously, an environmental-friendly electrolyte for the Cu plating would be more promising.

Room temperature ionic liquids are more advantageous media for the electrodeposition of metals and semiconductors, and have an unprecedented potential to revolutionize electroplating due to their wide electrochemical windows, extremely low vapour pressures, and numerous, only partly understood, cation/anion effects [15, 16]. As many ionic liquids are environmentally friendly, they are considered as suitable alternatives for many poisonous plating baths [17]. While the electrodeposition of Cu film was demonstrated by using air- and water-stable ionic liquids [18, 19], issues such as toxicity, availability and cost may limit their practical use [1]. Unlike the conventional ionic liquids, deep eutectic solvents (DESs) invented by Abbott and co-workers can be easily prepared at low cost and with high purity [20]. A series of metal films, such as Ni, Zn, Cr, and Cu were electrodeposited from the DES based solutions [21-23]. A recent work had demonstrated that nanocrystalline Ni films with an average grain size of about 6 nm was

Foundations: National Natural Science Foundation of China (51001089,51271169); Specialized Research Fund for the Doctoral Program of Higher Education of China (20100101120026)
Brief author introduction:谷长栋，(1978-)，男，副教授，主要从事电沉积薄膜和性能研究。E-mail: cdgu@zju.edu.cn

electrodeposited from a solution of nickel chloride salt in the typical DES based solvent of choline chloride (ChCl)─ethylene glycol (EG) at room temperature [12], while from the same solution flower-like Ni films with superhydrophobic surfaces were obtained but at a high temperature of about 90 °C [24]. Moreover, a series of Ni-Co alloy and porous Sn films were successfully electrodeposited from the DES based solutions [25, 26]. Abbott and co-workers thoroughly investigated the kinetics and thermodynamics of the electrodeposition of Cu and its composites from a solution of CuCl2·2H2O in either ChCl─urea or ChCl─EG based eutectic [1]. It was reported that bright Cu coatings and composite coatings of Cu with uniformly distributed Al2O3 and SiC particles could be electrodeposited from this novel DES-based plating baths [1].

In aqueous plating baths complexing agents and grain-refinement additives are usually used to produce a brighter and harder coating. However, researches on the effects of additives on the electrodeposition in the DES based solutions are limited [23, 27]. Abbott and co-workers' work has indicated that the additives in the DES based solutions would much influence the nucleation mechanism of zinc or nickel and the resultant morphologies. However, effects of additives on the microstructure and coating corrosion properties are still deficient. From the viewpoint of material applications, these characterizations are essential for the films fabricated from ionic liquids. Based on this thought, this work took a comparative study on the deposition mechanism, microstructure, and corrosion resistance of Cu films electrodeposited from the solution of CuCl2·2H2O in ChCl─EG based solvent without and with the additive of ethylene-diamine (EDA).

1 Experimental details

ChCl [HOC2H4N(CH3)3Cl] (AR, Aladdin), EG (AR, Aladdin) and EDA (AR, Sinopharm Chemical Reagent Co., Ltd.) were used as received. The eutectic solvent was formed by stirring the mixture of the two components in a mol ratio of 1 ChCl:2 EG at 80 °C until a homogeneous colourless liquid was formed. The base plating bath for Cu films is a solution of 0.45 mol/l CuCl2·2H2O in the above eutectic solvent. The additive of EDA was added to the base plating bath with a concentration of 1.36, 1.80 and 2.10 mol/l, respectively. The cathodic electrodeposition of copper was performed in a two electrode cell. The anode was copper-phosphorus alloy plate and the cathode was the polished brass foil (CuZn alloy). Copper films were electrodeposited at a constant voltage of -0.6 V and room temperature (25±3 °C) for 2 hours without stirring process. At last the newly obtained deposits were sequentially rinsed with methanol and deionized water.

Surface morphology of as-deposited Cu films was characterized by scanning electron microscopy (FE-SEM, Hitachi S-4800). Cross-sectional morphology of the Cu films was observed by an S-3400N SEM and chemical composition was analyzed with an X-ray energy dispersive spectroscope (EDS, BRUKER AXS) attached to this SEM. The cross section of Cu film was prepared by embedding the sample in epoxy resin and further by polishing it with abrasive cloths to a mirror-like finish surface. Crystalline structure of the film was studied by X-ray diffractometer (XRD, Rigaku D/max 2550PC, Japan) with a Cu target (λ=1.54056 Å) and a monochronmator at 40 kV and 250 mA with the scanning rate and step being 4°/min and 0.02°, respectively. The microstructure of the cross-sectional Cu film was also analyzed with a high resolution transmission electronmicroscope (HR-TEM, H-800). A cross sectional TEM sample was prepared by gluing the samples face-to-face with M-Bond 610 adhesive, and sections were cut with a diamond saw. Then the sample was ground and polished to a final thickness of approximately 5 μm. Finally, the sample was mounted to a TEM grid and ion-milled (Gantan 691) at gradually decreased voltages from 4.8 to 3.2 kV until a perforation formed.

Cyclic voltammetry of the plating bath and electrochemical measurements for the Cu films were carried out using an UI502X computer-based electrochemical Analyzer (LabNet, China). Cyclic voltammetry experiment was performed in a three electrode system consisting of a platinum microelectrode (0.25 cm^2), a platinum counter electrode and a silver wire quasi-reference electrode at ambient temperature (25±3 °C) and at various scan rates. Linear sweep voltammetry experiments were carried out in a 3.0 wt. % NaCl aqueous solution using a classic three-electrode cell with a platinum plate as counter electrode and a saturated calomel electrode (SCE, +245 mV vs SHE) as reference. During the potentiodynamic sweep experiments, the samples were first immersed into 3 wt.% NaCl solution for about 30 min to stabilize the open-circuit potential. Potentiodynamic curves were recorded by sweeping the electrode potential from a value of about 100 mV lower to a value of 200-300 mV greater than the corrosion potential, at a sweeping rate of 1 mV/s without the deaeration process. The log(i)–E curves were measured after the above potentiodynamic sweep experiments. The corrosion potential E_{corr} and corrosion current density i_{corr} were deduced from these log(i)–E curves by Tafel region extrapolation.

Headlines of diagram and table: the headline should be placed in the middle under the diagram, and above the table. The Chinese characters are in Song typeface, numbers and English are in Times New Roman, and Roman characters are in Symbol. Type size: 9 points.

2 Results and discussion

2.1 Stability of plating bath

Fig.1 Stability of the electrolyte for Cu electrodeposition. (A) Base electrolyte; (B) Base electrolyte after about 6 h electroplating process; (C)-(G) correspond to the base electrolyte with EDA additive of 0.1, 0.3, 0.6, 0.9, and 1.36 mol/l, respectively

The fresh base plating bath of 0.45 mol/l $CuCl_2{\cdot}2H_2O$ in ChCl-EG solvent is transparent and has a dark-orange color as shown in Figure 1A. Pure Cu films with a bright appearance can be easily electrodeposited from the fresh base electrolyte. However, after about 6 h of electrodeposition process in the base electrolyte, the color of the solution was changed to green-yellow and some undetermined green precipitate appeared at the bottom of the container (see Figure 1B), which indicates that the base electrolyte for Cu electrodeposition is not as stable as expected [1]. It should be noticed that the solution of nickel chloride salt in a ChCl-EG solvent is very stable for a long period of electroplating process [12, 24]. The invalidation of the Cu plating bath might be attributed to the electrochemical decomposition of chemical component in the ChCl-based solution [28]. Therefore, additives for complexing metal ions in the Cu base electrolyte seem to be necessary to constitute a stable DES-based plating bath for the Cu electrodeposition. In this study, EDA was chosen to represent a stronger nitrogen containing ligand for most transition metal ions. EDA was gradually added into the base plating bath and the color of the plating bath correspondingly changed from yellow to dark-blue, which indicates that EDA alters the Cu species presence in the solution. However, as indicated in Figure 1C, D, and E,

the more additive added, the more insoluble solids in the solution appeared. Strangely, when the concentration of EDA was further increased to 0.9 mol/l, the blue insoluble solids was abruptly reduced by comparing Figure 1E and F. No insoluble solid was found in the plating bath when the concentration of EDA was about 2 times as many as the concentration of $CuCl_2 \cdot 2H_2O$. As shown in Figure 1G, no any precipitation was found in the Cu plating bath with an additive of 1.36 mol/l. Moreover, the Cu plating bath with the additive of EDA is stable enough to undergo a long period of electrodeposition process. Therefore, in this study the concentration of EDA was chosen as 1.36, 1.80, and 2.10 mol/l to investigate the effect of EDA on the electrodeposition process of Cu. Clearly that the solution behavior in terms of complexation presented here suggests higher solubility for the $Cu(EDA)_2$ complex. However, the mechanism underlying the strange complexation is not clear now, and it is really an open question that deserves further investigation.

2.2 Cyclic voltammetry measurements

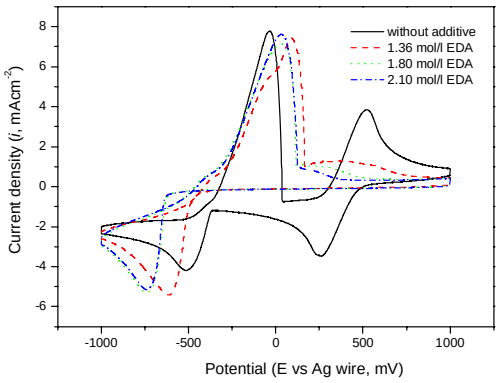

Fig. 2 Cyclic voltammogram at room temperature at 5 mV/s for 0.45 mol/l $CuCl_2 \cdot 2H_2O$ in 1:2 ChCl:EG and with different concentrations of additive (EDA).

Figure 2 compares the cyclic voltammetric response of the base plating bath (i.e. 0.45 mol/l $CuCl_2 \cdot 2H_2O$ in ChCl-EG solvent) in the absence and presence of EDA with a concentration of 1.36, 1.80, and 2.10 mol/l, respectively. The voltammograms obviously show the presence of cathodic and anodic peaks that correspond to deposition and redissolution. For the base plating bath, the voltammogram shows that there are two distinct reduction processes corresponding to the reversible Cu(II)/Cu(I) couple at the potential onset of +0.480 V followed by the reduction from Cu(I) to Cu(0) at -0.374 V, which is similar to Abbott and co-workers' work [1]. The latter process results in metallic copper deposition with a characteristic stripping response on the anodic scan. However, the addition of EDA to the base electrolyte has a marked effect on the cyclic voltammetry (Figure 2). Only one couple of redox process corresponding to the copper deposition and copper redissolution is observed. Moreover, three voltammograms present the characteristic crossover between the currents for the positive and negative sweeps, which suggests the presence of a nucleation and growth process [29]. Upon the introduction of 1.36 mol/l EDA to the base electrolyte, the onset of reduction is shifted about 82 mV cathodically to -0.456 V. Further increasing the concentration of EDA to 1.80 and 2.10 mol/l in the base electrolyte, respectively, the onsets of Cu reduction sequentially shifted cathodically to the similar value of -0.620 V, which suggests that in this system the EDA inhibits the initiation of Cu nucleation. Figure 2 also indicates that the presence of the additives alters both the Cu deposition and stripping processes. The major stripping peaks of Cu oxidation for the EDA modified electrolyte shift much anodically compared with the base electrolyte. This may indicate that the addition of EDA in the base electrolytes would produce a larger polarization. The difference in cyclic voltammograms should

account for the different morphology which is confirmed by the following SEM observations.

2.3 Surface morphology and chemical composition

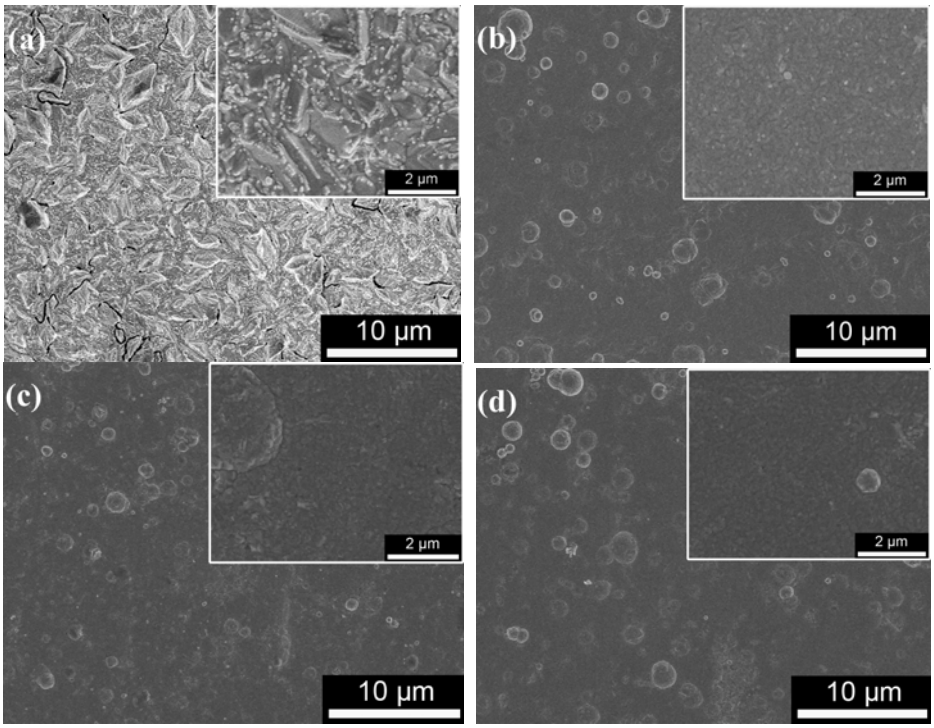

Fig.3 Surface morphologies of the electrodeposited Cu films from the Cu base plating bath (0.45 mol/l $CuCl_2 \cdot 2H_2O$ in 1:2 ChCl:EG) with different concentrations of EDA. (a) 0; (b) 1.36; (c) 1.80; (d) 2.10 mol/l. Insets are the corresponding magnified images

Figure 3 gives the typical surface morphologies of as-deposited Cu films from the base electrolyte in the absence (a) and presence of EDA with a concentration of 1.36 mol/l (b), 1.80 mol/l (c), and 2.10 mol/l (d), respectively. The insets are the corresponding magnified images. In the absence of EDA, the electrodeposited Cu film is characterized by a rough surface and larger grains with obvious edges as shown in Figure 3a. Some of about 100 nm sized grains preferentially were grown on the protrudent points of larger grains (Inset of Figure 3a). Cracks and holes along grain boundaries are observed on the Cu surface (Figure 3a). However, the surface morphologies of Cu films make a pronounced improvement when the modified electrolytes with the addition of EDA were used (Figure 3b-d). Smooth and compact surfaces with fine grain structures can be obtained in the electrodeposited Cu films from the modified electrolyte with the additive of EDA, which indicates that EDA might act as the grain finer for the electrodeposition. A few spherical grain clusters with diameters of 200-300 nm are scattered on the Cu surfaces. Moreover, it is found that the concentration of EDA has little effect on the surface morphologies of the electrodeposited Cu films. The EDS mapping analysis (not shown here) indicates only Cu is found in the Cu films shown in Figure 3.

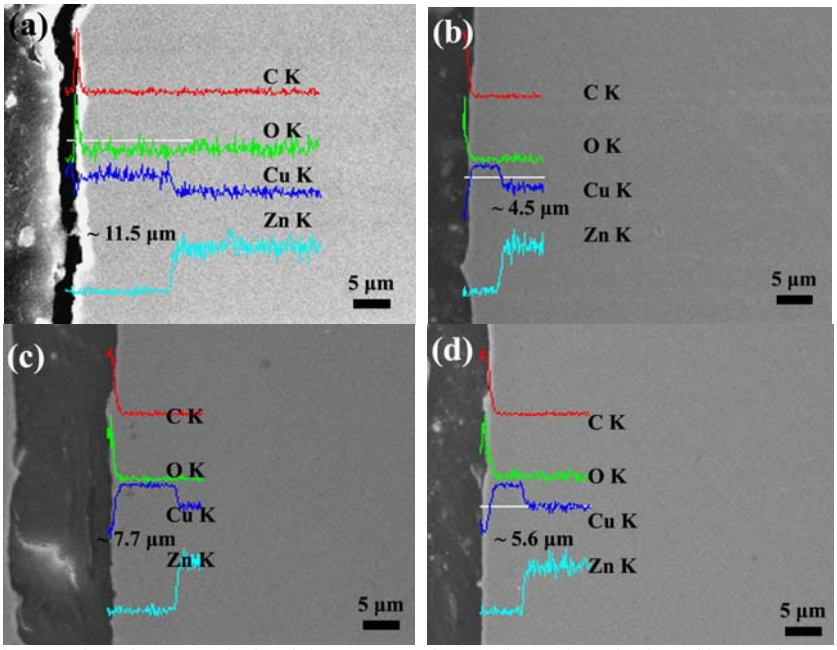

Fig. 4 SEM micrograph and EDS analysis of the cross-section of electrodepsoited Cu films on brass substrate from the DES-based electrolyte with different concentration of EDA. (a) 0; (b) 1.36 mol/l; (c) 1.80 mol/l; (d) 2.10 mol/l.

Figure 4 shows the SEM images incorporated with EDS analysises of the cross-section of electrodepsoited Cu films on brass substrates from the base electrolyte in the absence (a) and presence of EDA with a concentration of 1.36 mol/l (b), 1.80 mol/l (c), and 2.10 mol/l (d), respectively. It is hard to distinguish the film/substrate interface in the SEM images, which implies that the Cu films are tightly attached to the substrate. With the aid of EDS linear analysis as shown in Figure 4, the thickness of Cu films can be easily distinguished. The EDS signal of C and O shown in Figure 4 comes from the epoxy resin and the Zn is originated from the brass substrate. The Cu film electrodeposited from the base electrolyte has a thickness of about 11.5 µm (Figure 4a). However, the thicknesses of Cu films electrodeposited from the modified electrolyte with EDA are in the range of 4.5-7.7 µm, which is much thinner than the film obtained in the base electrolyte. It is further verified that the addition of EDA strongly inhibits the nucleation and growth of Cu deposits.

2.4 XRD analysis and TEM observations

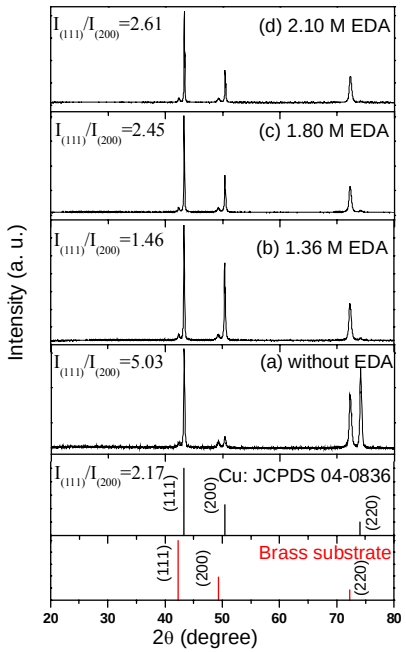

Fig. 5 XRD patterns of the as-deposited Cu films obtained from the base electrolyte (a: 0.45 mol/l $CuCl2{\cdot}2H2O$ in 1:2 ChCl:EG) and with EDA concentration of 1.36 (b), 1.80 (c), 2.10 mol/l (d), respectively. Standard XRD reports for Cu (JCPDS 04-0836) and brass substrate (CuZn alloy: JCPDS 00-050-1333) are also shown in this figure.

Figure 5 gives XRD patterns of the as-deposited Cu films obtained from the base electrolyte (a) and with different EDA concentrations (b-d). Standard XRD reports for Cu (JCPDS 04-0836) and brass substrate (CuZn alloy: JCPDS 00-050-1333) are also shown in this figure. In Figure 5, the peaks at 43.3°, 50.4°, and 74.1° are assigned to the face-centered cubic (fcc) Cu planes of (111), (200), and (220), respectively, which is well agree with the report of JCPDS 04-0836. The other peaks shown in Figure 5 are assigned to the substrate (JCPDS 00-050-1333). No other crystal phases are detected in the Cu electrodeposits. Interestingly, a strong (111) preferred texture is found in the Cu film electrodeposited from the base plating bath, showing a much higher peak intensity ratio of the (111) to (200) diffractions, i.e. $I_{(111)}/I_{(200)}=5.03$, than that from a polycrystalline Cu with randomly distributed grains ($I_{(111)}/I_{(200)}=2.17$), as indicated in Figure 5. However, for the Cu films from the 1.80 mol/l and 2.10 mol/l EDA addition electrolytes, the (111) texture becomes very weak (see Figure 5c and d). The disappearance of (111) texture in the Cu films obtained from the modified electrolytes indicates that the addition of EDA in the electrolyte leads Cu grains to a randomly distribution. Finer grain structure in the Cu films as shown in Figure 3 is also suggested to be responsible for the weakening of (111) preferred texture, which is further confirmed by TEM observations. Moreover, it seems that the $I_{(111)}/I_{(200)}$ decreased firstly and then increased with increasing concentration of EDA (Figure 5b, c, and d), which implies that the structure of the deposits may be manipulated by the concentration of EDA.

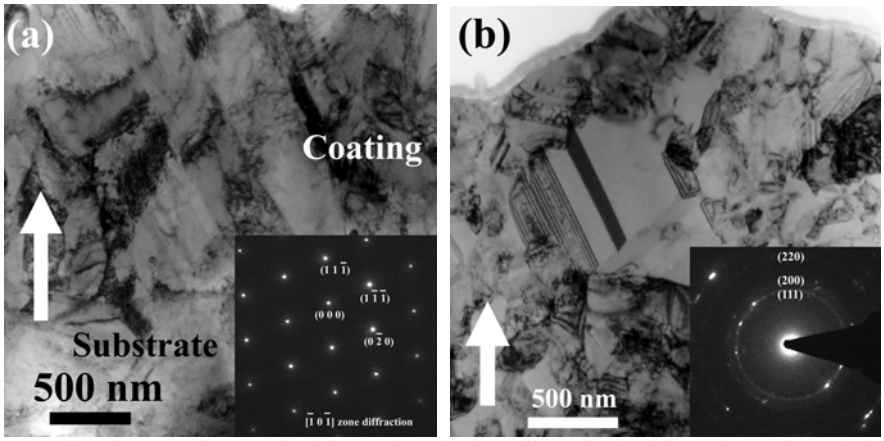

Fig. 6 Cross-sectional TEM micrograph of the as-deposited Cu films obtained from the Cu base plating bath (a) and with 1.36 mol/l EDA (b).The corresponding SAED patterns are shown as insets. Arrows indicate the growth direction of the deposits on the brass substrate.

Figure 6 shows the cross-sectional TEM micrograph of the as-deposited Cu films on brass substrate from the base electrolyte in the absence (a) and presence of EDA with a concentration of 1.36 mol/l (b), respectively. The insets are selected area electron diffraction (SAED) patterns corresponding to Figure 6a and b, respectively. As shown in Figure 6a, typically columnar grains nearly vertically grown from the substrate can be observed, which is in agreement with the (111) textures detected by XRD (Figure 5a). However, in the case of Ni electrodeposition, no columnar grains were formed in the cross-section of films [12]. The indexed spot of SAED patterns in the [011] beam direction in the inset of Figure 6a confirm the fcc structure of the Cu film with coarse grains, which is in a good agreement with the result of XRD. Upon the introduction of 1.36 mol/l EDA to the base electrolyte, the microstructure of Cu electrodeposits changes a lot as shown in Figure 6b. Most importantly, columnar grains disappear. The Cu grains show a bimodal grain size distribution that is some ultrafine grains with a size of about 80-100 nm are embedded in submicrometre-sized grains (500-700 nm). The cleaved facets in some larger grains should be resulted from the growth twins with a lamella thickness ranging from about 15 to 100 nm. Figure 6b also indicates that the modified Cu consists of irregular-shaped grains with random orientations (see the SAED patterns in the inset of Figure 6b). The ring-like patterns of the SAED also confirm the fine grain structure of the fcc Cu film. This characteristic of grain structure is expected to deliver an optimized mechanical property [8]. The TEM observations shown in Figure 6 are well consistent with the above SEM and XRD results (Figure 2 and 5).

2.5 Corrosion resistance property of the Cu films

Corrosion resistance of coatings is closely related to their microstructures. The microstructure variation of those Cu films obtained from different plating baths is expected to produce different corrosion resistance properties. Figure 7 gives the potentiodynamic polarization curves for the four Cu films in a 3.0 wt.% NaCl aqueous solution at room temperature without stirring. The anodic branch of polarization curve has the most important features related to the corrosion resistance. Corrosion potential E_{corr} and corrosion current density i_{corr} are derived from the potentiodynamic polarization curves and summarized in Table 1. The Cu film obtained from the base electrolyte has a E_{corr} of -0.209 V and a i_{corr} of 5.7×10^{-6} A cm^{-2}. However, the Cu films obtained from the modified electrolytes possess a little negatively shifted E_{corr} and decreased i_{corr} compared with the Cu film from the base electrolyte (see Figure 7 and Table 1). In a certain sense, the corrosion current density reflects the rate of corrosion of coatings [30]. The addition of EDA to the base electrolyte produces the fully dense Cu films, which has a positive effect on enhancing the

corrosion resistance of Cu deposits. Furthermore, the Cu films obtained from the modified electrolyte are readily to be passivated by comparing the curves in the Figure 7. An obvious passive phenomenon with a passive current density ranging from 9.5×10^{-6} to 1.4×10^{-5} A·cm^{-2} is found in the Cu films from the modified electrolyte while not found in that from the base electrolyte (see Table 1). At the critical potential E_{crit} of -0.128 V for 1.36 mol/l EDA addition, -0.106 V for the 1.80 mol/l EDA addition, and -0.096 V for 2.10 mol/l EDA addition, the passive films broke down, and the onset of pitting took place. The electrochemical behaviors of Cu films in this study are reproducible, which indicates that the presence of the EDA in the electrolytes may have a clear corrosion inhibiting influence for the deposits, with producing a compact and fine grained structure on the surfaces.

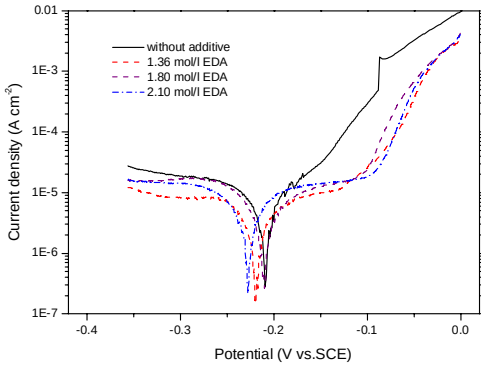

Fig. 7 Electrochemical polarization curves of the electrodeposited Cu films from the base electrolyte and with various concentration of EDA in 3.0 wt.% NaCl aqueous solution.

Tab. 1 Summary of the electrochemical measurements (Figure 7) of electrodeposited Cu films.

Concentration of EDA in the base electrolyte (mol/l)	Corrosion potential, E_{corr}/ V	Corrosion current density, i_{corr}/ A cm^{-2}	Passive current density, i_{corr}/ A cm^{-2}
0	-0.209	5.7×10^{-6}	/
1.36	-0.220	2.2×10^{-6}	9.5×10^{-6}
1.80	-0.210	2.7×10^{-6}	1.3×10^{-5}
2.10	-0.227	2.5×10^{-6}	1.4×10^{-5}

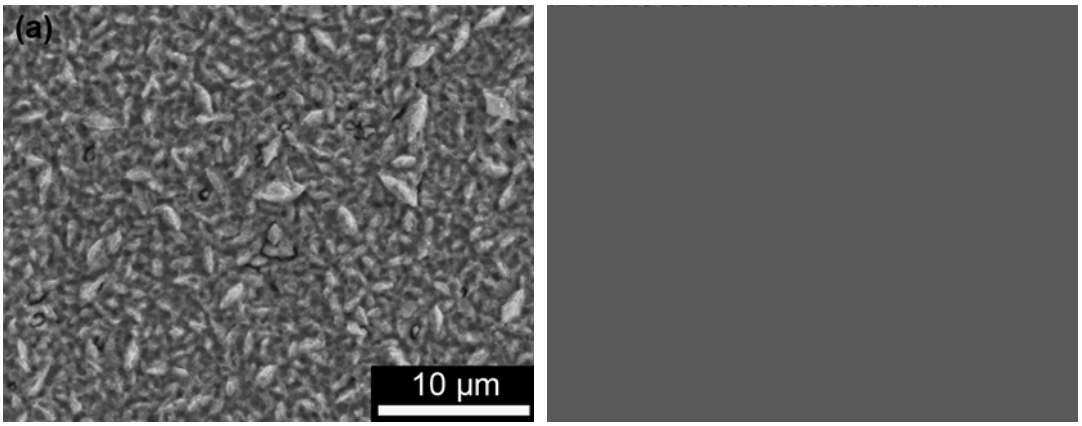

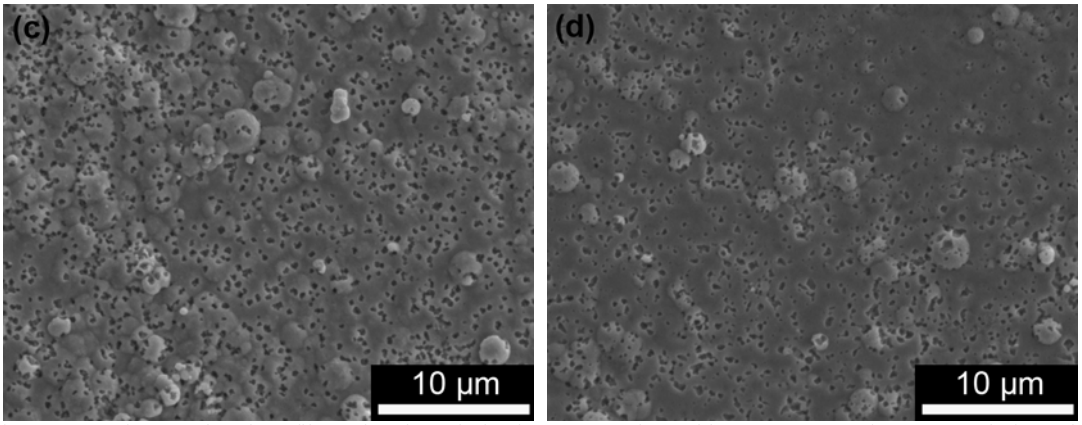

Fig. 8 SEM micrographs of Cu films after the polarization tests performed in 3.0 wt.% NaCl aqueous solution. The Cu films obtained from the base electrolyte (a) and with EDA concentration of 1.36 (b), 1.80 (c), 2.10 mol/l (d), respectively.

To explore the corrosion characteristics of Cu films in the 3.0 wt.% NaCl aqueous solution, the samples after the polarization tests of Figure 7 were examined using SEM and shown in Figure 8. Comparing Figure 8a with 3a, the Cu film obtained from the base electrolyte was severely corroded in the Cl^- containing aqueous solution, where a preferential etching along grain boundaries was recognized, resulting in the grooves in Figure 8a. EDS survey of the Cu film shown in Figure 8a indicated that a small quantity of O (about 2.56 wt.%) was detected on the surface, which might be that a weak oxide layer was formed during the polarization. However, this oxide layer should be not stable enough to contribute a passivation for the Cu film revealed by the potentiodynamic polarization curve (Figure 7). As shown in Figure 8b-c, there are plenty of corrosion pin-holes uniformly distributed on the surfaces of Cu films obtained from the modified electrolytes, which indicates that uniform corrosion occurs. According to the EDS analysis, only Cu was found on the films surfaces. Therefore, the passivation of the films from the modified electrolyte should be attributed to the fine grain structure and the low porosity in the films [10]. As discussed above, the addition of EDA leads to a finer grain structure of Cu deposits. The high surface fractions of grain boundaries and triple junctions of the fine grain structures could provide an increased number of preferential attack sites and therefore disperse the corrosion current density [10, 12]. So, the Cu films obtained from the modified electrolyte exhibit decreased corrosion current densities compared with the Cu film obtained from the base electrolyte.

3 Conclusion

Here, we took a comparative study on the deposition mechanism, microstructure, and electrochemical property of Cu electrodeposits from the base plating bath of $CuCl_2{\cdot}2H_2O$ in ChCl─EG based eutectic solvent with absence and presence of the additive of EDA. It was found that the base electrolyte was unstable for a long period of Cu electrodeposition process and the as-deposited Cu film consisted of typically columnar grains with a strongly (111) preferred texture. Upon the introduction of EDA to the base electrolyte, the nucleation and growth of Cu deposits were strongly inhibited, thus producing a much smooth and compact surface with finer grains. All electrodeposited Cu films from the ChCl─EG based electrolytes were pure Cu and had an fcc crystal structure revealed by EDS and XRD analysis, respectively. Potentiodynamic polarization measurements and SEM observations on the corroded surfaces indicated that the addition of EDA to the base electrolyte had a positive effect on enhancing the corrosion resistance of Cu deposits.

Acknowledgements

The work was supported by the National Natural Science Foundation of China (51001089, 51271169), the Specialized Research Fund for the Doctoral Program of Higher Education of China (20100101120026).

References

[1] A P ABBOTT, K El TTAIB, G FRISCH, K J MCKENZIE, K S RYDER.Electrodeposition of copper composites from deep eutectic solvents based on choline chloride[J]. Physical Chemistry Chemical Physics,2009, 11(21): 4269-4277.

[2] M CERISIER, K ATTENBOROUGH, J FRANSAER, C VAN HAESENDONCK, J P CELIS. Growth mode of copper films electrodeposited on silicon form sulfate and pyrophosphate solutions[J]. Journal of the Electrochemical Society, 1999,146(6): 2156-2162.

[3] D GRUJICIC,B PESSIC. Electrodeposition of copper: the nucleation mechanisms[J].Electrochimica Acta,2002,47(18): 2901-2912.

[4] V S DONEPUDI, R VENKATACHALAPATHY, P O OZEMOYAH, C S JOHNSON, J PRAKASH.Electrodeposition of copper from sulfate electrolytes -Effects of thiourea on resistivity and electrodeposition mechanism of copper[J].Electrochemical and solid state letters,2001,4(2):C13-C16.

[5] HUANG C A,WANG T H,T WEIRICH,V NEUBERT. Electrodeposition of a protective copper/nickel deposit on the magnesium alloy (AZ31)[J]. Corrosion Science,2008, 50(5): 1385-1390.

[6] S C TJONG,CHEN H.Nanocrystalline materials and coatings[J]. Materials Science and Engineering R, 2004,45: 1-88.

[7] LU L, SHEN Y F,CHEN X H,QIAN L H,LU K.Ultrahigh strength and high electrical conductivity in copper[J].Science,2004, 304(5669):422-426.

[8] WANG Y,CHEN M,ZHOU F,MA E.High tensile ductility in a nanostructured metal[J]. Nature,2002,419(6910):912-915.

[9] A ROBERTSON, U ERB,G PALUMBO.Practical applications for electrodeposited nanocrystalline materials[J].NanoStructured Materials,1999,12(5-8):1035-1040.

[10] GU C D,LIAN J S,HE J G,JIANG Z H,JIANG Q.High corrosion-resistance nanocrystalline Ni coating on AZ91D magnesium alloy[J]. Surface Coating and Technology,2006,200(18-19):5413-5418.

[11] I ROY, YANG H W, L DINH, I LUND, J C EARTHMAN, F A MOHAMED.Possible origin of superior corrosion resistance for electrodeposited nanocrystalline Ni[J].Scripta Materialia, 2008,59(3):305-308.

[12] Gu C D, YOU Y H,YU Y L,QU S X.Microstructure, nanoindentation, and electrochemical properties of the nanocrystalline nickel film electrodeposited from choline chloride-ethylene glycol[J]. Surface and Coatings Technology,2011,205(21-22): 4928-4933.

[13] K JOHANNSEN, D PAGE,S ROV.A systematic investigation of current efficiency during brass deposition from a pyrophosphate electrolyte using RDE, RCE, and QCM[J]. Electrochimica Acta,2000, 45(22-23): 3691-3702.

[14] A N CORREIA, M X FACANHA,P DE LIMA-NETO.Cu-Sn coatings obtained from pyrophosphate-based electrolytes[J]. Surface and Coatings Technology,2007, 201(16-17): 7216-7221.

[15] M ARMAND, F ENDRES,D R.MACFARLANE,H OHNO,B SCROSATI.Ionic-liquid materials for the electrochemical challenges of the future[J]. Nature Materials,2009, 8(8): 621-629.

[16] F ENDRES.Ionic liquids: Solvents for the electrodeposition of metals and semiconductors[J]. Chemphyschem,2002, 3(2): 144-154.

[17] S Z El ABEDIN, M POLLETH,S A MEISS,J JANEK,F ENDRES.Ionic liquids as green electrolytes for the electrodeposition of nanomaterials[J].Green Chemistry,2007, 9(6): 549-553.

[18] Chen P Y,SUN I W. Electrochemical study of copper in a basic 1-ethyl-3-methylimidazolium tetrafluoroborate room temperature molten salt[J]. Electrochimica Acta,1999, 45(3): 441-450.

[19] K MURASE,K.NITTA,T.HIRATO,Y AWAKURA.Electrochemical behaviour of copper in trimethyl-n-hexylammonium bis((trifluoromethyl)sulfonyl)amide, an ammonium imide-type room temperature molten salt[J].Journal of Applied Electrochemistry,2001, 31(10): 1089-1094.

[20] A P ABBOTT, D. BOOTHBY,G CAPPER,D L DAVIES,R K RASHEED. Deep eutectic solvents formed between choline chloride and carboxylic acids: Versatile alternatives to ionic liquids[J]. Journal of the American Chemical Society, 2004,126(29): 9142-9147.

[21] A P ABBOTT, K S RYDER,U KONIG.Electrofinishing of metals using eutectic based ionic liquids[J]. Transactions of the Institute of Metal Finishing,2008, 86(4): 196-204.

[22] A H WHITEHEAD, M POLZLER,B GOLLAS.Zinc electrodeposition from a deep eutectic system containing choline chloride and ethylene glycol[J].Journal of the Electrochemical Society,2010, 157(6): D328-D334.

[23] A P ABBOTT, J C BARRON,G FRISCH,K S RYDER,A F SILVA.The effect of additives on zinc electrodeposition from deep eutectic solvents[J]. Electrochimica Acta,2011, 56(14): 5272-5279.

[24] Gu C D,TU J P.One-step fabrication of nanostructured Ni film with lotus effect from deep eutectic solvent[J].Langmuir,2011, 27(16): 10132-10140.

[25] Gu C D,MAI Y J,ZHOU J P,YOU Y H,TU J P. Non-aqueous electrodeposition of porous tin-based film as an

anode for lithium-ion battery[J].Journal Of Power Sources,2012, 214(0): 200-207.
[26] YOU Y H,GU C D,WANG X L,TU J P.Electrodeposition of Ni-Co alloys from a deep eutectic solvent[J]. Surface and Coatings Technology,2012, 206(17): 3632-3638.
[27] A P ABBOTT, K El TTAIB,K S RYDER,E L SMITH.Electrodeposition of nickel using eutectic based ionic liquids[J]. Transactions of the Institute of Metal Finishing,2008,86(4): 234-240.
[28] K HAERENS,E MATTHIJS,K BINNEMANS,B VAN DER BRUGGEN.Electrochemical decomposition of choline chloride based ionic liquid analogues[J].Green Chemistry,2009, 11(9): 1357-1365.
[29] F R BENTO,L H MASCARO.Electrocrystallisation of Fe-Ni alloys from chloride electrolytes[J].Surface and Coatings Technology,2006, 201(3-4): 1752-1756.
[30] GU C D,LIAN J S,LI G Y,NIU L Y.High corrosion-resistant Ni–P/Ni/Ni–P multilayer coatings on steel[J].Surface and Coatings Technology,2005,197(1): 61-67.

含乙二胺的深共熔溶剂中电沉积铜薄膜的微观结构与腐蚀性能研究

谷长栋，尤益辉，王秀丽，涂江平
（浙江大学材料科学与工程学系，杭州 310025）

摘要：本文系统研究了乙二胺对深共熔溶剂中电沉积铜薄膜的微观结构和腐蚀性能的影响规律。分析了乙二胺对深共熔溶剂中电沉积铜薄膜的沉积机理。实验发现当深共熔溶剂型铜电镀液中不含有乙二胺时，电镀过程不稳定，得到的铜薄膜具有典型柱状晶结构，而且表面较粗糙。通过向铜电镀液中加入一定量的乙二胺，电镀液形成稳定的体系。同时乙二胺有效地抑制了铜晶粒的形核，从而得到表面光滑致密的铜薄膜。透射电子显微镜观察表明电沉积柱状晶组织减弱，铜晶粒大小趋于纳米化，分布均匀。电化学极化性能测试表明乙二胺电镀液体系中获得的铜薄膜具有较低的腐蚀电流，耐蚀性较高。

关键词：电沉积；离子液体；铜；添加剂；耐腐蚀
中图分类号：TB31